Fabrication of a novel silica PLC hybrid integrated triplexer

Junyi Li (李俊一)*, **Junming An (安俊明)**, **Yuanda Wu (吴远大)**, **Jianguang Li (李建光)**, **Hongjie Wang (王红杰)**, and **Xiongwei Hu (胡雄伟)**

Optoelectronics Research and Development Center, Institute of Semiconductors, Chinese Academy of Sciences, Beijing 100083, China

**E-mail: junyi_lee@semi.ac.cn*

Received November 19, 2009

A new-style silica planar lightwave circuit (PLC) hybrid integrated triplexer, which can demultiplex 1490-nm download data and 1550-nm download analog signals, as well as transmit 1310-nm upload data, is presented. It combines SiO_2 arrayed waveguide gratings (AWGs) with integrated photodetectors (PDs) and a high performance laser diode (LD). The SiO_2 AWGs realize the three-wavelength coarse wavelength-division multiplexing (CWDM). The crosstalk is less than – 40 dB between the 1490- and 1550-nm channels, and less than – 45 dB between 1310- and 1490- or 1550-nm channels. For the static performances of the integrated triplexer, its upload output power is 0.4 mW, and the download output photo-generated current is 76 μA. In the small-signal measurement, the upstream –3-dB bandwidth of the triplexer is 4 GHz, while the downstream –3-dB bandwidths of both the analog and digital sections reach 1.9 GHz.

OCIS codes: 250.3140, 130.3120, 130.0250, 130.0130.
doi: 10.3788/COL20100806.0588.

Access network speed is a bottleneck that must be improved to increase available bandwidth. At present, fiber-to-the-home (FTTH) communication is poised to become a major technology for the next generation access networks. The optical bidirectional transceiver (TRx) module is considered to be the key component in realizing FTTH networks. In recent years, an optical triplex TRx module that can transmit 1310-nm upload data, as well as receive 1490-nm download data and 1550-nm download video signals for cable television (TV) applications, has become the focus of some researchers in this field. The triplex TRx module, which consists of a thin-film filter (TFF), a high-performance laser diode (LD), and photodetectors (PDs) in the transistor outline, has already been produced. However, this has been proven to be a costly alternative. One realistic method of achieving a cost-effective TRx module is to use silica planar lightwave circuit (PLC) hybrid integration technology[1−3].

The conventional wavelength-division multiplexers (WDMs) formed on a PLC platform are TFF-embedded WDMs[4−6] that generally experienced difficulties in forming a narrow trench and embedding the TFF chip into the trench without tilting. To address this problem, a WDM structure, in which the TFF chip is attached to the sidewall of the PLC platform, has been applied to a diplex TRx module using two wavelength bands[7]. However, the costs of the TFF and the coupling between TFF and waveguide are still high. To further reduce the costs, we replace TFF with a SiO_2 arrayed waveguide grating (AWG) filter[8−10] and use ultraviolet adhesive and active alignment technique to fabricate a new-style triplexer. To our knowledge, no other study has been reported on this type of structure. In this letter, we provide a detailed description of the structure and module performances of the triplexer.

Figure 1 shows a schematic of the triplex TRx module. A 1310-nm spot-size converted (SSC) Febry-Perot LD on the LD carrier was integrated into the PLC platform to form a transmitter (Tx). Two receiving surface-illuminated PDs in pairs with a light detecting diameter of 50 μm each were vertically bonded to the PD carrier to face the sidewall of the PLC platform[7,11], forming a digital and analog receiver (Rx). On the PDs carrier, a transimpedance amplifier (TIA), some microstrip lines, and glass ceramics were placed to form an electronic circuit configuration; this will amplify the weak current generated by the 1490-nm digital PD. The SiO_2 AWG filter realized the coarse wavelength-division multiplexing (CWDM) by transmitting 1310-nm upstream data through port b, thereby receiving 1490-nm downstream data and 1550-nm downstream analog signals through ports a and c, respectively. The silica waveguides had an index contrast of 0.75% and a core size of 5.5×5.5 (μm) to maintain single mode conditions. To suppress the electrical crosstalk between the LD and PDs, we arranged the output ports a and c at the right facet, and the output b at the down facet. The fiber and the LD and PDs carriers were integrated onto the PLC platform using the ultraviolet adhesive.

Figure 2(a) shows the sketch map of the coupling between the LD and PLC. As can be seen, the 250 × 240 μm SSC-LD is bonded on the glass ceramics on silicon. The p and n electrodes of the SSC-LD are then injected into the current by two glass ceramics. The SSC-LD and the PLC are integrated using active alignment technique and ultraviolet adhesive whose refractive index is 1.56. Meanwhile, Fig. 2(b) shows the sketch map of the

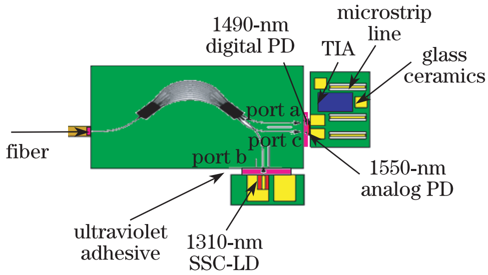

Fig. 1. Schematic configuration of the triplex TRx module.

coupling between the PDs and PLC. The 600×300 (μm) PDs in pairs without separating, which are vertically bonded to the sidewall of the PD carrier to receive light from the waveguide, are also employed to form a digital and an analog Rx. The center distance of two 50-μm light detecting areas is 300-μm, so the waveguide spacing is also designed to the same distance to align a single PD. The p electrode of each PD is also led by the glass ceramics, while the n electrode is led by silicon coated with Au. The unpackaged hybrid integrated triplexer chip is shown in Fig. 3.

The AQ6370B optical spectrum analyzer was used to test the optical performances of the triplexer. The three-wavelength narrowband optical sources were multiplexed to a fiber output using a multiplexer. Figure 4(a) shows the spectral responses of the 1310-, 1490-, and 1550-nm optical sources. As can be seen, the three optical waves are transported by a fiber to the input of the SiO_2 AWG filter. The output spectra of ports a and c are shown in Figs. 4(b) and (c), respectively. As shown in Fig. 4(b), the output power for the 1490-nm wave is – 8 dBm, while those for the 1550- and 1310-nm waves are – 49 and – 54 dBm, respectively. The crosstalk is less than – 40 dB between the 1490- and 1550-nm waves, while that between the 1310- and 1490-nm waves is less than – 45 dB.

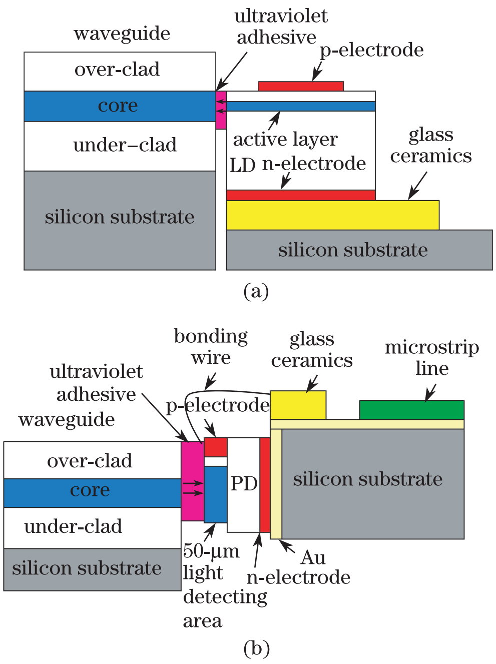

Fig. 2. Sketch maps of the coupling between (a) the LD and waveguide, (b) the PDs and waveguide.

Fig. 3. Unpackaged triplexer chip.

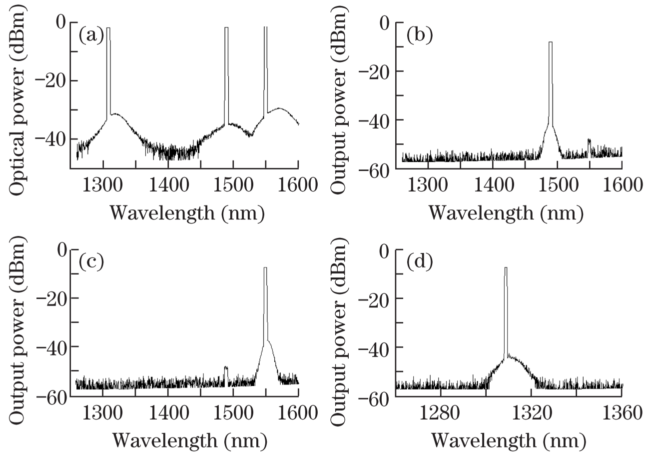

Fig. 4. (a) Spectral response of the optical source; (b) output spectrum of port a; (c) output spectrum of port c; (d) upstream output spectrum of port b.

Figure 4(c) confirms the crosstalk between the 1490- and 1550-nm waves; it also shows that the crosstalk is less than – 45 dB between the 1310- and 1550-nm waves. Figure 4(d) shows the upstream output spectrum of port b. From these graphs, we can infer that the SiO_2 AWG filter has a low optical crosstalk.

As for the static performances of the integrated triplexer, an upload output power of about 0.4 mW is obtained when the LD is provided with 15-mA bias current, and the laser efficiency is about 0.0267 mW/mA. However, the slope efficiency of the bare LD chip is about 0.33 mW/mA; thus, the entire loss reaches about 11 dB. The whole loss factor includes the optical coupling loss between the fiber and the AWG, the propagation loss in the AWG, and the AWG-LD excess coupling loss caused by the misalignment. After testing, the propagation loss in the silica AWG was found to be 5 dB. The coupling of the fiber and AWG had a large loss reaching 7 dB; in addition, the optical coupling loss was 2 dB and the AWG-LD excess coupling loss was 4 dB. We used a refractive index matching liquid to improve the coupling efficiency. The download output photo-generated current was 76 μA when the input 1550-nm wavelength power was 1 mW and the reverse bias voltage applied to PD was 2.6 V. The analog Rx responsivity value of 0.076 A/W corresponded to a loss of 10.5 dB compared with the reference responsivity of 0.85 A/W in the case of the best alignment between the fiber and the PD carrier. With the aforementioned loss of 7 dB in the coupling of the fiber and AWG, the AWG to PD carrier coupling loss can be presumed to be 3.5 dB, which is also large. We believe this is due to a position error in a slant diced AWG sidewall. The digital Rx had the same problem.

The vector network analyzer (VNA) was used to perform the small-signal measurement. The small-signal measurement schematics of the Tx and Rx of the hybrid integrated triplexer are shown in Figs. 5(a) and (b), respectively. Figure 5(c) shows the frequency responses of the Tx of the triplexer for different bias currents. We determined that the upstream – 3-dB bandwidth of the triplexer was 4 GHz, and that in-band flatness was better when the bias current was 15 mA compared with others. The downstream – 3-dB bandwidth of the analog Rx of triplexer was 1.9 GHz (Fig. 5(d)). On the other hand,

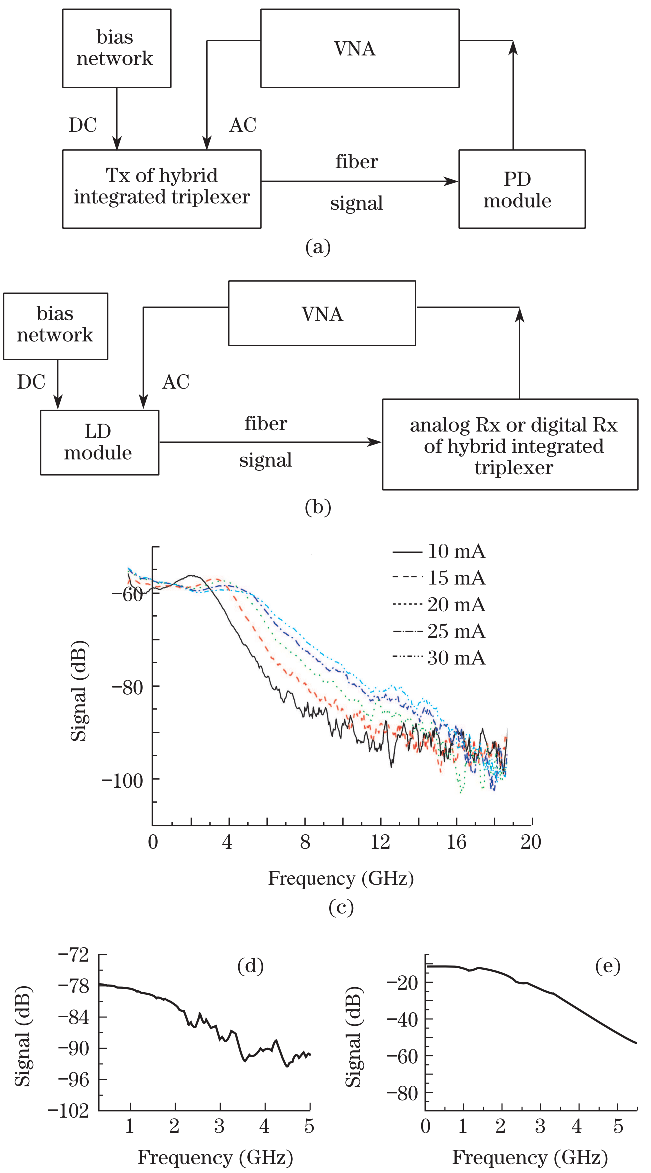

Fig. 5. Small-signal measurement schematics of (a) Tx and (b) Rx of the hybrid integrated triplexer; (c) frequency responses of the Tx of the triplexer for different bias currents; frequency responses of (d) the analog Rx and (e) the digital Rx of the triplexer. DC: direct current; AC: alternating current.

the − 3-dB bandwidth of the digital Rx of triplexer was also 1.9 GHz when the optical source was provided with a 50-mA bias current (Fig. 5(e)). The difference between Figs. 5(d) and (e) is that the commercial TIA (gain 24 kΩ, data rates 1.25 Gb/s, and root-mean-square (RMS) noise 130 nA) realizes signal amplification. From these graphs, we can infer that the TRx has good signal bandwidth performances.

In conclusion, a PLC hybrid integrated triplexer with PD and LD carriers is fabricated. The active alignment technique and ultraviolet adhesive are employed to couple the SiO_2 AWG filter with the PDs and LD. The triplexer has low optical crosstalk and wide signal bandwidth, although its coupling loss is still high. In future studies, the coupling efficiency could be raised by using refractive index matching liquid and by reducing the position errors.

This work was supported by the National “863” Project of China (Nos. 2006AA03Z420 and 2007AA03Z420) and the National Natural Science Foundation of China (Nos. 60776057, 60837001, and 60877014).

References

1. M. Kawachi, IEEE Proc.-Optoelectron. **143,** 257 (1996).
2. J.-U Shin, D.-J. Kim, S.-H. Park, Y.-T. Han, H.-K. Sung, J. Kim, and S.-J. Park, ETRI Journal **24,** 398 (2002).
3. M. Ishii, Acta Opt. Sin. (in Chinese) **23,** (suppl.) 199 (2003).
4. H. Yanagawa, T. Ochiai, H. Hayakawa, and H. Miyazawa, J. Lightwave Technol. **7,** 1646 (1989).
5. T. Hashimoto, T. Kurosaki, M. Yanagisawa, Y. Suzuki, Y. Akahori, Y. Inoue, Y. Tohmori, K. Kato, Y. Yamada, N. Ishihara, and K. Kato, J. Lightwave Technol. **18,** 1541 (2000).
6. T. Hashimoto, A. Kanda, R. Kasahara, I. Ogawa, Y. Shuto, M. Yanagisawa, A. Ohki, S. Mino, M. Ishii, Y. Suzuki, R. Nagase, and T. Kitagawa, in *Proceedings of 2003 Electronic Components and Technology Conference* 280 (2003).
7. M. Oguro, A. Goto, N. Kitamura, Y. Fukutomi, Y. Sakamoto, T. Masuta, and T. Tamura, in *Proceedings of 2002 Electronic Components and Technology Conference* 305 (2002).
8. T. Lang, J.-J. He, and S. He, IEEE Photon. Technol. Lett. **18,** 232 (2006).
9. Q. Liu, W. Ma, W. Wang, G. Hu, and Y. Xu, Acta Opt. Sin. (in Chinese) **24,** 1265 (2004).
10. Y. Wu, P. Lu, and D. Liu, Chinese J. Lasers (in Chinese) **30,** 521(2003).
11. Y. Doi, M. Ishii, S. Kamei, I. Ogawa, S. Mino, T. Shibata, Y. Hida, T. Kitagawa, and K. Kato, Electron. Lett. **39,** 1603 (2003).